Global NEST Journal, Vol 20, No X, pp XX-XX

Kinetics study of the ability of compost material for removing Cu^{2+} from wastewater

Benjreid R.[1*], Matouq M.[2], Al-Alawi M.[1] and György F.[1]

[1]Szent István University, Institute of Environmental Science, Department of Soil Science and Agricultural Chemistry Gödöllő, Páter Károly u. 1. H-2100, Hungary

[2]Al-Balqa Applied university, Faculty of Engineering Technology, Chemical Engineering Department, Amman, POBox 4486, 11131, Jordan

Received: 13/08/2018, Accepted: 17/09/2018, Available online: 26/09/2018

*to whom all correspondence should be addressed: e-mail: bengreed@yahoo.com

https://doi.org/10.30955/gnj.002865

Abstract

The objective of this study is to examine the ability of a compost material for removing Cu^{2+} from aqueous solutions with different parameters using continuous fixed-bed column. Compost was characterized by using Fourier transform infrared spectroscopy which revealed that the metal binding is mainly contributed to the ionic interaction of the metal cations with the carboxyl groups in the hemic substances. Scanning electron microscope images were utilized for morphological analysis of the adsorbent and has revealed that the changes in compost composition could be related to the mechanism of metal binding. Energy dispersive X-ray spectroscopy was used before and after the metal had loaded and gives a good evidence on compost adsorption of Cu^{2+} and the metals have its involvement in the interaction in the adsorption process. The influence of the initial Cu^{2+} concentration, flow rate, bed heights of the column, and ion exchange have been studied in this research. The adsorption kinetic models have revealed that the behaviour of the Cu^{2+} adsorption is dependent on rate of concentration, flow rate, and bed heights.

Keywords: Wastewater treatment, compost, heavy metal removal, adsorption kinetics, Cu ions removal, kinetics models.

1. Introduction

Heavy metals are major environmental pollutants and their destructive is a challenging of increasing significance for environmental surroundings. The contamination of aquatic environments has increased due to the discharging of destructive and no-biodegradable compounds present in the wastewater of several industrial activities. It has been reported in numerous studies that such heavy metals have high potential for inducing severe damage on human health and natural aquatic environment due to their predisposition to bio-accumulate and permanence (Feng *et al.,* 2009). In recent decades, the annual global release of heavy metal reached 22,000 tons (metric tons) for cadmium, 939,000 tons for copper, 783,000 tons for lead and 1,350,000 tons for zinc (Singh *et al.,* 2003). Consequently, it became very important to remove such contaminants from industrial wastewater before they are discharged into the environment. While a number of researchers have attempted to resolve this problem through the use of different technologies, an efficient and cost effective approach for heavy metal removal is still remains a big challenge. Adsorption has been recognized as an effective process in most of the industrial water and wastewater treatment. Moreover, adsorption methods using the fixed bed system has shown a trend for removal of heavy metal and simple in construction. It can be conducted in single or in series columns at same time. In addition, the operation is preferred when dealing with a large volume of wastewater as the process is conducted continuously and is controllable. This, in turn, the application is more practical and economical for an industrial scale operation. In an effort to develop a useful, easy to use, eco-friendly and low-cost application, the study conducted attempted the removal of heavy metal by compost material. Compost has several benefits, such as improving soil fertility, soil structure, increasing plant fertility, increasing water absorption capacity. Besides its use as fertilizer, compost can also be applied as a heavy metal adsorbent. Specifically, relatively little attention has been devoted to studying the effects of compost in contentious mode of heavy metal removal via adsorption. It would thus be of interest to study whether these materials will be feasible for metal removal. Copper is applied in several industries and can be serious problem when discharged into the environment without treatment, excessive amount are poisonous to humans and animals. Health effects caused by cupper well reported in literature. Therefor this paper aims to evaluate the adsorption of Cu^{2+} by using compost material as an adsorbent application.

2. Materials and methods

2.1. Preparation of adsorbent

Garé compost was provided by laboratory of biocombustibles from Szent Istvan University, Gödöllő (Hungary). Garé is a communal sewage sludge, slurry mud and chicken manure with straw, its chemical composition evaluated by SEM and depicted in Table 1. The compost was ground and sieved into fractions below 2 mm. The fractions collected below mesh size of 2 mm were designated for the characterization and adsorption investigations without any pre-treatment. The particular weight was 5, 10, and 15 g and has packed accordingly to the column's heights and act as a fixed bed in the column. Previous research has investigated the adsorption process in batch experiments using different heavy metals as an adsorbed onto same compost and the results give a good removal of such metals using compost (Benjared *et al.,* 2016).

2.2. Fixed bed column construction

The glass columns were 30 cm long, 1.2 cm internal diameter with porous ending at the bottom. The column packed with desired amount of compost representing the height of the bed column with two supporting layers of glass wool at the top and the bottom. Columns positioned vertically and adsorption tests were performed in continuous down flow method besides the experiments were conducted at room temperature. The schematic diagram is illustrated in Figure 1. Wastewater kept in an overhead container and the only driving force of the solution through the column is the gravity and it is manually controlled for its flow operation. A flow control valves used to adjust the flow at 4 and 8 mL/min. The initial heavy metal concentration of 20 and 100 mg/L of Cu^{2+} was prepared using analytical grade ($CuSO_4 5H_2O$) (Merck, Germany) by dissolving the required quantity of copper sulphate in distilled water. It was further diluted to obtain standard solutions. 1000 mL of aqua solution field the on overhead tank and then charged into fixed bed columns. The samples were collected at different time intervals to analyze Cu^{2+} traces using atom absorption spectrophotometer.

3. Result and discussion

3.1. Analysis and characterization of compost

3.1.1. Scanning electron microscopy (SEM)

The surface morphology of the compost was examined by SEM before and after Cu^{2+} was loaded. The scanning electron microscope was set at x35 and x50 magnification, while the accelerated voltage was set at 5 kV in order to obtain high-resolution micrographs at different adsorbent spots. Figure 2a, shows how an irregular surface, which is heterogeneously shaped and cracked probably favours the sorption of Cu^{2+} on different parts of the adsorbent; making it a propitious adsorption technique. From Table 1 it was observed that after adsorption of Cu^{2+}, ions of other elements have been reduced or diapered such as Na, Cl. Amount of exchangeable cations Na^{+} was reduced after metal adsorption (Galindo *et al.,* 2013; Vieira *et al.,* 2014). The appearance of Cu feature on the surface of adsorbent indicates that the adsorbent studied was able to bind metal ions. Moreover it can be said that other elements have involved in the ion exchange process with the Cu^{2+} ions. From Table 1 the analysis of adsorbent also indicated that carbon was a major component in compost, followed by oxygen and nitrogen. Because of the heterogeneous structure and composition of the compost, the chemical elemental analysis was expected to show the chemical constitutes which could influence the heavy metal adsorptive capacity of the adsorbent. Figure 2b, reveals that the morphological changes in raw compost, is due to adsorption of Cu^{2+} on the compost surface.

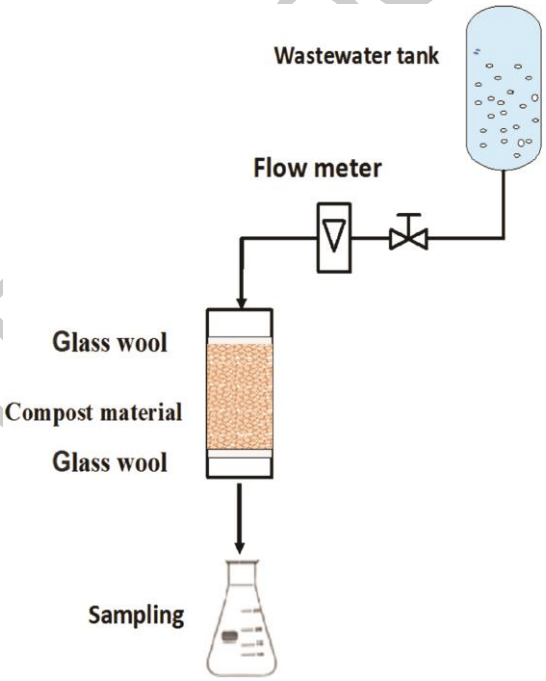

Figure 1. Experimental set up

3.1.2. Energy dispersive X-ray spectroscopy (EDX)

EDX analysis provided direct confirmation for the copper adsorption onto the compost material. The samples were coated with gold prior to analysis to avoid electron charging. Resulting interaction with metal ions, the presences of Cu^{2+} can be observed in EDX spectrum of the compost. The EDX spectrum before and after exposure with Cu^{2+}. The disappearance of some metal presence after metal ion adsorption can be attributed to ion-exchange mechanism, this behaviour has also reported by (Kamari *et al.,* 2014). The appearance of Cu^{2+} features can be observed on EDX spectrum at different energy values indicate that the adsorption of Cu^{2+} was able to bind metal ions on compost surface.

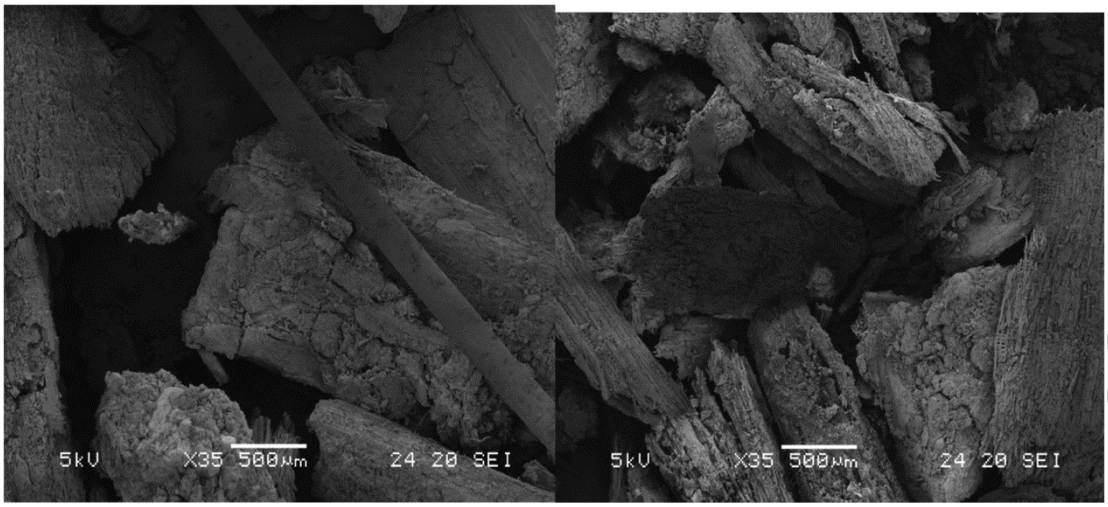

(a)

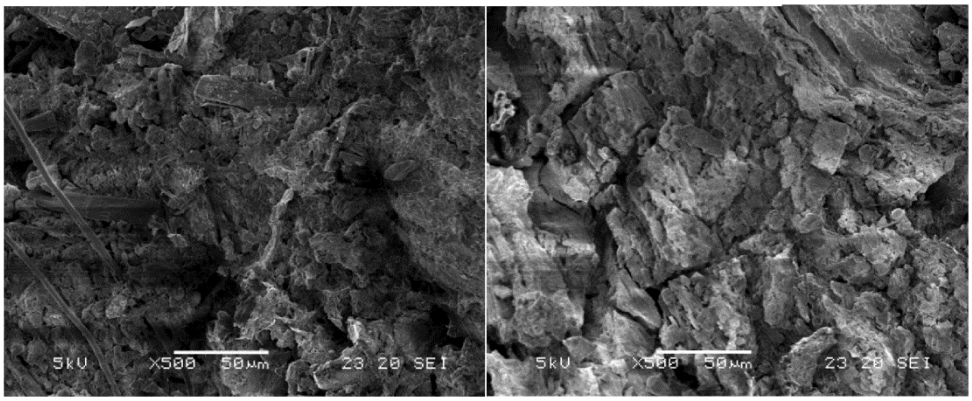

(b)

Figure 2. Scanning electron micrograph (SEM) of compost before (a) and after (b) Cu loading

3.1.3. Fourier transform infrared spectroscopy (FTIR)

While the characteristic peaks of the main organic components are present in all spectra, no significant differences can be observed: the different ratio of the various peaks (indicating different composition from the major organic substances) is probably simply related to the very heterogeneous compost sample as very low amounts of sample (less than 10 mg) is required for a pellet. Moreover, there were no major changes such as the appearance or disappearance of peaks was observed in the treated samples when compared to the references. Supposing that the metal binding is mainly due to the ionic interaction of the metal cations with the carboxyl groups in the humic substances, a shift in the ratio of the peaks related to the protonated and dissociated carboxyl groups could indicate the metal binding. However, the peak related to the protonated carboxyl around 1720 cm^{-1} is not observed even in the reference, probably due to the salt formation occurring with other present cations (such as Na, K etc.), and during the treatment only the change of the cation occurs; thus, the metal binding has no noticeable effect on the spectra. Figure 3 indicated the peak of 3400 cm^{-1} is wide band related to the OH and NH groups and 2930 cm^{-1} C-H stretching in the -CH2- groups; 1630 C=O bond (mainly in the carboxyl groups), though the relative wide peak probably indicates the presence of C=C and amide groups as well, 1430 related to the O-H and C-O bonds, then 1380 probably CH bonds, although other peaks related to other groups such as nitrate may also be present, which is indicated by the non-steep curve at lower wavelengths. 1070, 1030 relatively wide band related to the C-O-C bonds in various polysaccharides, the size and relativity of the two peaks is simply related to the differences in the polysaccharide ratio (such as the starch, cellulose, etc. content; the presence of clay minerals may also affect the band). There are likely more characteristic peaks, which overlap with the most intensive ones mentioned above, thus making their identification difficult in a complex sample like compost, which contains a wide variety of organic compounds.

Table 1. Chemical composition of raw compost and after loaded with Cu

Sample	Raw compost		Raw compost		Cu loaded		Cu loaded	
Magnification	x35		x50		x35		x50	
Element	At. ratio	wt%	At. ratio	wt%	At. ratio	wt%	At. Ratio	wt%
C	42.478	33.232	44.96	36.711	44.323	35.685	41.372	33.629
N	10.427	9.513	10.054	9.574	10.438	9.8	11.433	10.838
O	39.605	41.275	40.439	43.985	39.964	42.861	42.915	46.467
Na	0.243	0.364	0.287	0.449				
Mg	0.484	0.767	0.349	0.577	0.188	0.306	0.154	0.253
Al	0.739	1.298	0.528	0.968	0.721	1.304	0.753	1.376
Si	2.338	4.277	1.565	2.988	2.342	4.409	2.15	4.087
P	0.598	1.207	0.31	0.653	0.314	0.652	0.269	0.563
S	0.274	0.573	0.24	0.522	0.184	0.396	0.125	0.272
Cl	0.135	0.311	0.084	0.202				
K	0.613	1.562	0.298	0.793	0.1	0.263	0.098	0.259
Ca	1.841	4.807	0.733	1.996	1.022	2.747	0.495	1.344
Fe	0.224	0.816	0.153	0.583	0.273	1.021	0.18	0.678
Cu					0.131	0.558	0.055	0.235

3.2. Adsorption kinetics studies for bed column

3.2.1. Mathematical description

The performance of the bed column system can be estimated using the shape of the breakthrough curve attained from the plot of C_{eff}/C_o contrary to time t, where C_{eff} and C_o are the effluent and influent concentrations. The adsorbed metal ion concentrations in the column are observed by a plot of the adsorbed metal concentration, C_{ad} = (1) or normalized concentration defined as the ratio of effluent metal concentration to influent concentration (C_{eff}/C_o) as a function of time or volume of effluent V_{eff}. The essential dynamics for column demonstration at various operating a breakthrough curve study are the bed height, flow rate, and initial inlet concentration. The effects of these factors on the profile of the breakthrough curve and column performance were studied and illustrated in Table 2.

$$C_{ad} = \text{Inlet concentration}(C_o) - \text{Outlet concentration}\ (C_{eff}) \quad (1)$$

$$V_{eff}\ (mL) = Q_{total} \quad (2)$$

where Q = Volumetric flow rate (mL/min) t_{total} = Total flow time (min)

$$q_{total}(mg) = \frac{Q}{1000} = \frac{Q}{1000}\int_{t=0}^{t=t_{total}} C_{ad}\,dt \quad (3)$$

$$q_{eq}\left(\frac{mg}{g}\right) = \frac{q_{total}}{X} \quad (4)$$

The metal removal percentage was determined from the relationship (5):

$$\%R = [(C_o - C_{eff})Q.t/mt] \times 100 \quad (5)$$

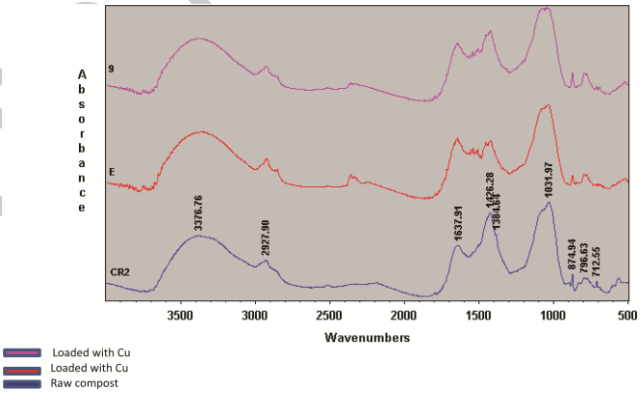

Figure 3. FTIR spectra of raw compost and Cu (II) loaded

3.2.2. Effect of initial inlet concentration on breakthrough curves

The effect of the initial inlet concentration on breakthrough curves was evaluated using 20 and 100 mg/L of Cu^{2+} inlet concentration solutions, while setting up the bed height at 2.4, 3.1 and 6.5 cm of absorbent respectively, the flow rate was manipulated at 4 mL/min and 8 mL/min. Table 2 is demonstrating the results obtained from the column. The breakthrough times of these curves decrease, and the curves dispersed and emerged slowly with increasing initial inlet concentration as demonstrated in Figure 4 at 20 mg/L concentration this effect was also observed by (Abdolali *et al.,* 2017). Higher removal percentage was observed with the decrease of inlet concentration (Oguz *et al.,* 2014). Both q_{eq} and q_{total} increased considerably by the increase of inlet concentration. q_{total} increased from 19.77 mg at Cu^{2+} concentration of 20 mg/L to 95.12 mg when the inlet concentration was 100 mg/L. q_{eq} increased from 3.88 mg/g to 17.55 mg/g at 20 mg/L and 100 mg/L respectively. Similar tendency has been reported by other researchers

(Martín *et al.,* 2016). This increase in the IE capacity could be explained by the fact that a higher influent Cu^{2+} concentration results in a higher driving force for the transfer process to overcome the mass transfer resistance (Sun *et al.,* 2014).

Table 2. Mathematical description of column parameters at various operating conditions

Flow rate (min/L)	Bed Height (cm)	Concentration (mg/L)	Amount (g)	q_{total} (mg)	q_{eq} (mg/g)	(%)
4	1.1	20	5	19.17	3.84	96
4	2	20	10	19.55	1.95	98
4	3.1	20	15	19.78	1.31	99
8	1.1	20	5	17.68	3.53	88
8	2	20	10	18.76	1.87	94
8	3.1	20	15	19.3	1.28	97
4	1.1	100	5	78.24	15.6	78
4	2	100	10	85.86	8.58	86
4	3.1	100	15	95.1	6.34	95
8	1.1	100	5	75.61	15.1	76
8	2	100	10	83.19	8.31	83
8	3.1	100	15	89.89	5.99	90

3.2.3. Effect of inlet flow rate on adsorption

Table 2 shows the column parameters at various operating conditions and its effect on adsorption process. This table also gives the removal percentage of ions at different operation conditions. Figure 5, demonstrate the breakthrough curve which became steeper and elevated when the flow rate changed from 4 to 8 mL/min, similar observation noticed by (Gong *et al.,* 2015) for removal of Cu^{2+} by biosorption onto coconut shell in fixed-bed column systems. At higher flow rate, it takes additional time for the bed to get saturated; whereas for lower flow rate there was sufficient time for the Cu^{2+} solution to get adsorbed on adsorbent. The column performed well at the lowest flow rate (Ozdemir *et al.,* 2009; Uddin *et al.,* 2009). The percentage of Cu^{2+} removal also decreases with increasing in flow rate and higher removal percentage occurred at slower flow rate. Table 2 shows the effect of flow rate on the adsorption capacity (q_{total}) and equilibrium adsorption (q_{eq}). When the flow rate rise, both q_{total} and q_{eq} decreases, similar observation has been observed by (Luo *et al.,* 2011; Riazi *et al.,* 2016), however q_{eq} was not reported with significant effect considerably. At higher flow rate, residence time of effluent in the bed is low. This is due to a decrease in contact time between the metal ions and the compost at higher linear flow rates. As the adsorption rate is controlled by intra-particulate diffusion, an early breakthrough occurs leading to a low bed adsorption capacity (Taty-Costodes *et al.,* 2005).

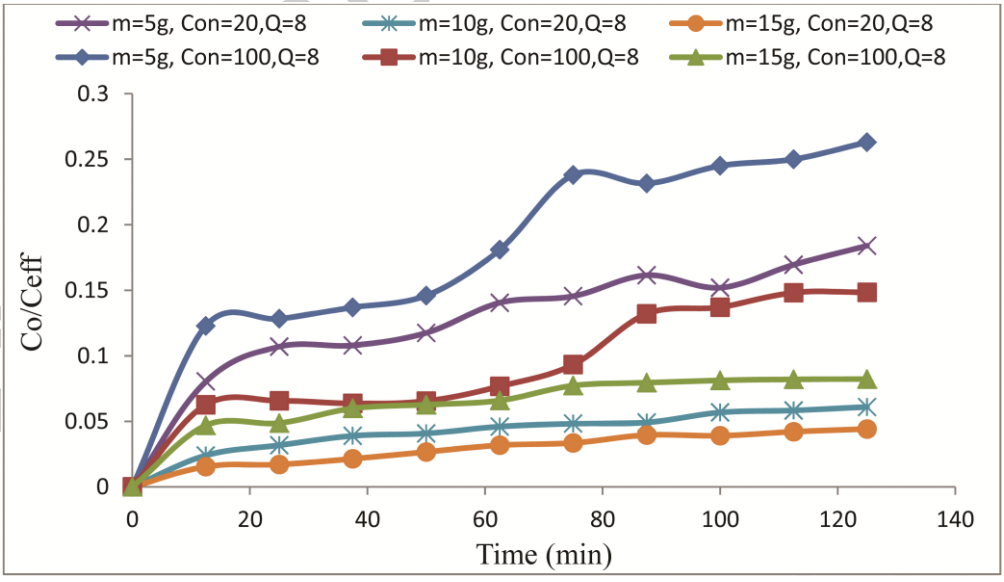

Figure 4. Effect of concentration 20, 100 mg/L at different bed heights, flow rate 8 mL/min

3.2.4. Effect of bed depth on breakthrough curves

The breakthrough curves at different bed height (2.4, 3.1 and 6.5 cm) are shown in Figure 6, using a constant influent concentration of 20 with a flow rate of 4, it is clear that the shape and slope of curve is changing with the variation of the bed depth. The breakthrough time increases at higher bed depth of adsorbent. The slope of the breakthrough curve decreases with the increasing in bed height, which result in a higher mass transfer zone (Ahmad and Hameed, 2010). The column parameters

obtained from effect of bed height is listed in the Table 2. According to Table 2, when the bed height increases, the removal percentage increases and the maximum adsorption capacity of the column is also increased, similar trend was observed by (Jain *et al., 2013;* Mishra *et al., 2016*). A correlation is found between the reduction of bed height and the lower retention of metallic ions in consequence of this is because the adsorbent has insufficient contact time to attract the adsorbate Cu^{2+}.

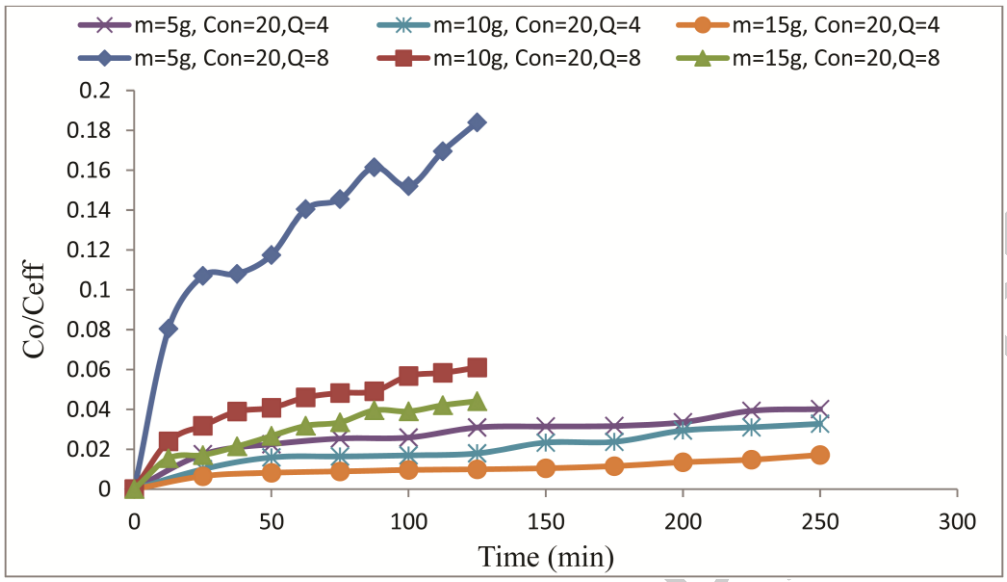

Figure 5. Effect of flow rate at 20 mg/L concentration at different bed heights, flow rate 4 and 8 mL/min

3.3. Breakthrough curves and kinetics modelling

In order to study the effect of the fixed bed column performance and to scale it up for industrial applications, three models investigated here and its implication. Adams–Bohart, Yoon–Nelson and Thomas models are used to analyse the behaviour of adsorbent–adsorbate adsorption in this research.

3.3.1. Adams–Bohart model

The Adams–Bohart adsorption model was applied to experimental data for the description of the initial part zone of the breakthrough curve. Plotting ln C_o/C_{eff} against t, using linear regression analysis on all breakthrough curves have ben plotted, the respective values of k_{AB} and N_0 were calculated and presented in Table 3. This model assumed that the biosorption rate is proportional to the residual capacity of the solids and the concentration of the sorbent substances (Calero *et al.,* 2009).

The Adams–Bohart is given in equation 6 as:

$$\ln\left[\frac{C_0}{C_{eff}}\right] = k_{AB}C_0 t - \frac{K_{AB}N_0 Z}{U_0} \quad (6)$$

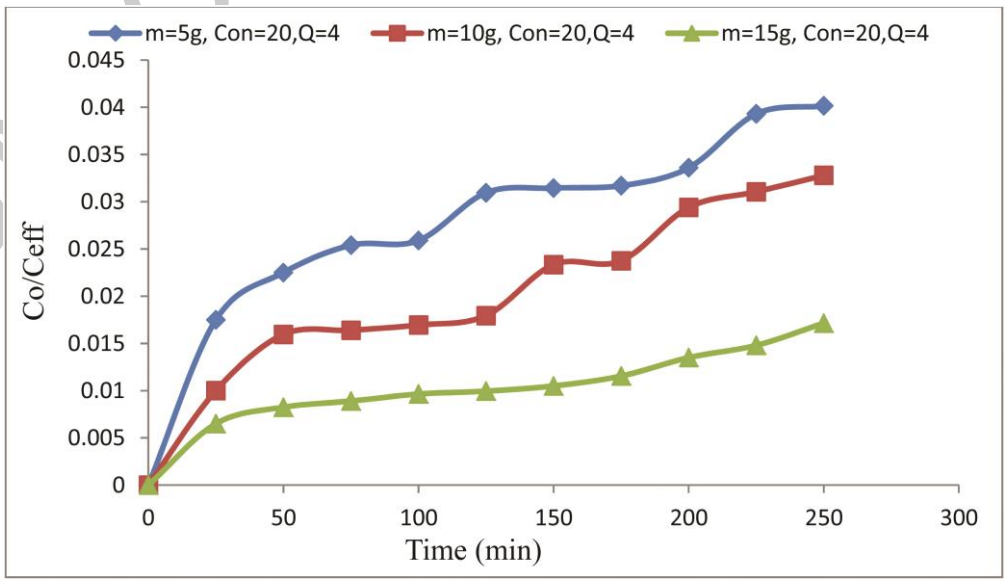

Figure 6. Effect of bed height at concentration 20 mg/L and 4 mL/min flow rate

Where C_o = influent concentration (mg/L); C_{eff} = effluent concentration (mg/L); k_{AB} = adsorption rate coefficient (L/mg/min); N_0 = adsorption capacity coefficient (mg/L); Z = bed depth (cm); N_0 = linear velocity (cm/min); and t = time (min). The amount of metal concentration adsorbed mg/g is calculated through the factor N_0 (adsorption capacity coefficient in mg/L). The kinetic constant values of k_{AB} and N_0 are determined from the slope and intercept of ln (C_0/C_{eff}) versus *t* and are listed in Table 4. The adsorption rate coefficient k_{AB} decreases as the increasing in the influent concentration from 0.000235 to 0.000032 as given in Table 3. The adsorption capacity coefficient (N_0) increases with the increase of the influent concentration from 45.5 to 351 mg/L, similar trend observed by (Bulgariu *et al.,* 2013). These results are accounted for on the basis that the greater availability of solute molecules on an adsorbent surface will affect higher uptake of Cu^{2+} molecules by unit mass of adsorbent. When the concentration is increasing, more solute molecules form greater concentration gradients, which ultimately reduce the adsorption rate coefficient. The adsorption rate coefficient k_{AB} is an indication of volume of influent treated by unit amount of adsorbent at unit time. When the flow rate increased from 4 to 8 mL/min the adsorption rate coefficient increased and N_0 decreased, this is in agreement with (Cheraghi *et al.,* 2016), the decrease in adsorption capacity is because of the lower residence time of solute in the column. Both k_{AB} and N_0 did not show any precise tendency with the changes of bed heights.

3.3.2. Thomas model kinetics

This model expressed through the second-order law of kinetic reaction without the presence of axial dispersion even when the bed depth was at the minimum and the breakthrough occurred immediately after the flow started as indicated by (Apiratikul *et al., 2008*). The Thomas equation is given by equation 7 as:

$$\ln\left[\frac{C_0}{C_{eff}}-1\right]=1+\frac{k_{thqo}m}{Q}-k_{th}q_0t \qquad (7)$$

Where C_0 is the initial metal concentration (mg/L), C_{eff} is effluent Cd^{2+} concentration (mg/L), at time t, k_{th} is Thomas model constant, L/min.mg. q_0 is maximum Cu^{2+} adsorption capacity (mg/g), m is mass of the adsorbent (g) and Q is flow rate (ml/min). The kinetic coefficient k_{th} and the adsorption capacity of the column q_0 can be determined from a plot of ln [C_o/C_{eff} - 1] against *t* at a given flow rate using linear regression. Thomas model aims at calculating the adsorption rate constant of the solid phase concentration of the metals on the adsorbent from the continuous mode studies. From results of Thomas model it clear that values of R ranges from 0.90 to 0.97. It can be observed from the Table 3, that the Thomas constant decreases with the increasing of the initial Cu^{2+} concentration from 0.000185 to 0.000037 at 20, 100 mg/L respectively, this is in a good agreement with (Aksu *et al., 2004*). In addition, q_0 increased from 10.3 to 49.5 mg/g to 20, 100 mg/L respectively. The appearance of such results are due to the driving force for adsorption concentration differences between the solute on the adsorbent and the solute in the solution. In consequence, this high driving force is a result of the higher Cu^{2+} concentration, which in turn, resulted in better column performance. This behaviour can be attributed to the increases in concentration that leads to increase in driving force for adsorption and will increase it. It can be observed that with the increases in flow rate, the maximum adsorption capacity is decreased and the coefficient K_{th} will also increase. This is because the residence time for solute in the bed is less, a similar trend was observed by (Sarma *et al., 2008*). Overall the value of q_0 decreased with increase in bed height and corresponding K_{th} values increased in general, this is in agreement with (Baral *et al.,* 2009). This is because, at higher bed heights, more reactive sites were available and driving force for adsorption increased.

3.3.3. Yoon–Nelson kinetic model

The Yoon–Nelson model is based on the assumption that the rate of adsorption is decreasing in the probability of adsorption, of adsorbate molecules, and is proportional to the probability of the adsorbate adsorption and the adsorbate breakthrough on the adsorbent (Han *et al.,* 2008). The values of (k_{YN}) and τ are determined from the slope and intercept of ln(C_0/(C_0-C_{eff})) versus *t* and the results are given in Table 6. The Yoon Nelson model is given in equation (8).

$$\ln\left[\frac{C_0}{C_0-C_{eff}}\right]k_{YN}t-\tau k_{YN} \qquad (8)$$

The time required for 50% adsorbent breakthrough (τ), decreases from 285, 250, 333 to 212, 185, 101 min on increasing the initial metal concentration from 20 to 100 mg/L when the bed height set at 2.4, 3.1 and 6.5 cm respectively. In addition, it decreases from 303, 208, 263 to 135,129,100 min on the increasing flow rate from 4 to 8 mL/min, which can be attributed to the rapid saturation of bed with higher flow rates along, this is in a good agreement with the results obtained by (Acheampong *et al.,* 2013). The increases in k_{YN} is in parallel with the increase of concentration and flow rate, however there is no specific trend with increasing of bed heights. Furthermore, k_{YN} is in general is increasing with the increases of bed height as depicted in Table 3. However, the values of τ are found to be higher in most cases than the *t* value at 50% breakthrough experimentally that observed under all conditions of evaluation, this is also in good agreement with previous studies (Víctor-Ortega *et al., 2016*).

Table 3. Parameters predicted by the Thomas, Adams Bohart, and Yoon Nelson Models parameters

Column Parameters				Thomas Parameters			Bohart Parameters			Nelson Parameters		
C_0 (mg/L)	Weight (g)	Bed heights (cm)	Q (min/mL)	q_0 (mg/g)	k_{th} (mL/min.m)	R^2	K_{AB} (L/min.mg)	N_0 (mg/g)	R^2	K_{YN} (min^1)	τ (min)	R^2
20	5	2.4	4	10.3	0.0002	0.92	0.000185	103.64	0.91	0.0033	303	0.92
20	10	3.1	4	7.59	0.0002	0.9	0.00026	49.92	0.92	0.0048	208	0.93
20	15	6.5	4	4.46	0.00025	0.93	0.00014	66.88	0.92	0.0038	263	0.96
20	5	2.4	8	10.3	0.00037	0.92	0.00051	29.48	0.93	0.0074	135	0.92
20	10	3.1	8	7.49	0.000385	0.9	0.000425	22.74	0.98	0.0077	129	0.9
20	15	6.5	8	4.46	0.0005	0.93	0.00038	18.84	0.9	0.01	100	931
100	5	2.4	4	49.5	0.000037	0.93	0.000073	377.04	0.92	0.0037	270	0.89
100	10	3.1	4	27.1	0.000044	0.97	0.000044	335.66	0.92	0.0044	400	0.97
100	15	6.5	4	35.5	0.000025	0.95	0.000033	384.51	0.96	0.0025	104	0.9
100	5	2.4	8	35.3	0.000096	0.91	0.000086	244.82	0.97	0.0096	95	0.91
100	10	3.1	8	22.8	0.000105	0.9	0.000116	130.14	0.96	0.0105	227	0.9
100	15	6.5	8	27.8	0.000058	0.9	0.000165	79.31	0.91	0.0058	174	0.9

4. Conclusions

The continuous down flow process designed in this study for adsorption using compost in order to remove the cupper ions has a good potential to remove heavy metals from wastewater in practical application. The compost materials used for cleaning the water polluted from Cu^{2+} could adsorb practically from 80 up to 98% at different operating conditions. It is also observed that the metal removal varied with varying initial metal concentration, bed height and effluent flow rate. In addition, these factors have shown its impacts on the adsorption process, breakthrough curve, percentage removal and adsorption capacity. The results of this study suggest that an adsorption system of utilizing copper ions using compost can be an economically feasible technique for the treatment of heavy metals in aqueous solution. The column parameters showed the major influences in the column performance and optimum operation factors that contributed to the effective removal of the metal ions. Experimental data embodied from breakthrough curves revealed up to 17.55 mg/g maximum Cu^{2+} adsorption capacity onto compost material. Moreover, a remarkable increases is observed in the Cu^{2+} equilibrium uptake efficiency with the escalation of the inlet Cu^{2+} ion concentration. The column behaviors can be predicted and assumed for further design implications and improvement works through the models applied in this study. Thomas model gives a good fit for the experimental data, at all the parameters examined, providing the necessary information about the dynamic behaviour of the Cu^{2+} adsorption process for appropriate column design and operation with high correlation coefficients values compared with Boahrt Adams and Yoon Nelson models. The FT-IR, SEM-EDX methods are an efficient techniques for investigating the physico-chemical characters concerning the compost and the process of adsorption before and after the metal loaded. EDX findings proves that the copper ions are efficiently removed by the adsorbent, the features of Cu^{2+} can be observed on EDX spectrum at different energy values. The compost in this study is capable to adsorb Cu^{2+} at different conditions designated on bed column. In addition, compost is very effective and environmentally friendly adsorbent which can be used in wastewater treatment without any chemical treatment.

References

Abdolali A., Ngo H., Guo W., Zhou J., Zhang J., Liang S., Chang S., Nguyen D., and Liu Y. (2017), Application of a breakthrough biosorbent for removing heavy metals from synthetic and real wastewaters in a lab-scale continuous fixed-bed column. *Bioresource Technology*, **229**, 78-87, doi:10.1016/j.biortech.2017.01.016

Acheampong M., Pakshirajan K., Annachhatre A. and Lens P. (2013), Removal of Cu(II) by biosorption onto coconut shell in fixed-bed column systems. *Journal of Industrial and Engineering Chemistry,* **19**, 841-848, doi:10.1016/j.jiec.2012.10.029

Ahmad A. and Hameed B. (2010), Fixed-bed adsorption of reactive azo dye onto granular activated carbon prepared from waste. *Journal of Hazardous Materials,* **175**, 298-303, doi:10.1016/j.jhazmat.2009.10.003

Aksu Z. and Gönen F. (2004), Biosorption of phenol by immobilized activated sludge in a continuous packed bed: Prediction of breakthrough curves. *Process Biochemistry,* **39**, 599-613, doi:10.1016/S0032-9592(03)00132-8

Apiratikul R. and Pavasant P. (2008), Batch and column studies of biosorption of heavy metal by Caulerpa lentillifera. *Bioresource Technology*, **99**, 2766-2777.

Baral S., Das N., Ramulu T., Sahoo S., Das S. and Chaudhury G. (2009), Removal of Cr(VI) by thermally activated weed Salvinia cucullata in a fixed-bed column. *Journal of Hazardous Materials,* **161**, 1427-1435. doi:10.1016/j.jhazmat.2008.04.127

Benjared R. and Füleky G. (2016), Cleaning heavy metal pollution of wastewater with compost application. Proceedings, Lviv, Ukraine, 6th International youth forum science "LITTERIS ET ARTIBUS", November, 24-26 (2016) 498-501

Bohart G. and Adams E. (1920), Some aspects of the behavior of charcoal with respect of chlorine. *Journal of the American Chemical Society,* **42**, 523-544. http://dx.doi.org/10.1021/ja01448a018

Bulgariu D. and Bulgariu L. (2013), Sorption of Pb(II) onto a mixture of aldgae waste biomass and anion exchanger resin

in a packed-bed column. *Bioresource Technology*, **129**, 374-380, doi:10.1016/j.biortech.2012.10.142

Calero M., Hernainz F., Blazques G., Tenorio G. and Martin-Lara M.A. (2009), Study of Cr (III) biosorption in a fixed-bed column. *Journal of Hazardous Materials,* **171**, 886-893. https://doi.org/10.1016/j.jhazmat.2009.06.082

Cheraghi E., Ameri E. and Moheb A. (2016), Continuous biosorption of Cd(II) ions from aqueous solutions by sesame waste: thermodynamics and fixed-bed column studies. *Desalination and Water Treatment*, **57**, 6936-6949. doi:10.1080/19443994.2015.1012744

Feng C., Guo X. and Liang S. (2009), Adsorption study of copper (II) by chemically modified orange peel. *Journal of Hazardous Materials,* **164**, 1286-1292. doi: 10.1016/j.jhazmat.2008.09.096

Galindo L., Neto A., Silva M. and Vieira M. (2013), Removal of Cadmium(II) and Lead(II) ions from aqueous phase on sodic bentonite. *Materials Research*, **16**, 515-527, doi:10.1590/S1516-14392013005000007

Gong J., Zhang Y., Jiang Y., Zeng M., Cui Z., Liu K., Deng C., Niu Q., Deng J. and Huan S. (2015), Continuous adsorption of Pb(II) and methylene blue by engineered graphite oxide coated sand in fixed-bed column. *Applied Surface Science*, **330**, 148-157, doi:10.1016/j.apsusc.2014.11.068

Han R., Ding D., Xu Y., Zou W., Wang Y., Li Y. and Zou L. (2008), Use of rice husk for the adsorption of congo red from aqueous solution in column mode. *Bioresource Technology*, **99**, 2938-2946, doi:10.1016/j.biortech.2007.06.027

Jain M., Garg V. and Kadirvelu K. (2013), Cadmium(II) sorption and desorption in a fixed bed column using sunflower waste carbon calcium-alginate beads. *Bioresource Technology*, **129**, 242-248, doi:10.1016/j.biortech.2012.11.036

Kamari A., Yusoff S., Abdullah F. and Putra W. (2014), Biosorptive removal of Cu(II), Ni(II) and Pb(II) ions from aqueous solutions using coconut dregs residue: Adsorption and characterisation studies. *Journal of Environmental Chemical Engineering*, **2**, 1912-1919, doi:10.1016/j.jece.2014.08.014

Luo X., Deng Z., Lin X. and Zhang C. (2011), Fixed-bed column study for Cu2+ removal from solution using expanding rice husk. *Journal of Hazardous Materials,* **187**, 182-189, doi:10.1016/j.jhazmat.2011.01.019

Martín-Lara M., Blázquez G., Calero M., Almendros A. and Ronda A. (2016), Binary biosorption of copper and lead onto pine cone shell in batch reactors and in fixed bed columns. *International Journal of Mineral Processing,* **148**, 72-82, doi:10.1016/j.minpro.2016.01.017

Mishra A., Tripathi B. and Rai A. (2016), Packed-bed column biosorption of chromium(VI) and nickel(II) onto Fenton modified Hydrilla verticillata dried biomass. *Ecotoxicology and Environmental Safety*, **132**, 420-428. doi:10.1016/j.ecoenv.2016.06.026

Oguz E. and Ersoy M. (2014), Biosorption of cobalt(II) with sunflower biomass from aqueous solutions in a fixed bed column and neural networks modelling. *Ecotoxicology and Environmental Safety*, **99**, 54-60, doi:10.1016/j.ecoenv.2013.10.004

Ozdemir O., Turan M., Turan A., Faki A. and Engin A. (2009), Feasibility analysis of color removal from textile dyeing wastewater in a fixed-bed column system by surfactant-modified zeolite (SMZ). *Journal of Hazardous Materials,* **166**, 647-654, doi:10.1016/j.jhazmat.2008.11.123

Riazi M., Keshtkar A. and Moosavian M. (2016), Biosorption of Th(IV) in a fixed-bed column by Ca-pretreated Cystoseira indica. *Journal of Environmental Chemical Engineering*, **4**, 1890-1898. doi:10.1016/j.jece.2016.03.017

Sarma R., Kumar J.P. and Pakshirajan K. (2015), Batch and Continuous Removal of Copper and Lead from Aqueous Solution using Cheaply Available Agricultural Waste Materials. *International Journal of Environmental Research*, **9**, 635-648.

Singh O., Labana S., Pandey G., Budhiraja R. andd Jain R. (2003), Phytoremediation: an overview of metallic ion decontamination from soil. *Applied Microbiology and Biotechnology*, **61**, 405-412. doi:10.1007/s00253-003-1244-4

Sun X.F., Imai T., Sekine M., Higuchi T., Yamamoto K., Kanno A., and Nakazono S. (2014), Adsorption of phosphate using calcined Mg3-Fe layered double hydroxides in a fixed-bed column study. *Journal of Industrial and Engineering Chemistry*, **20**, 3623-3630, doi:10.1016/j.jiec.2013.12.057

Taty-Costodes V., Fauduet V., Porte C. and Ho Y. (2005), Removal of lead (II) ions from synthetic and real effluents using immobilized Pinus sylvestris sawdust: Adsorption on a fixed-bed column. *Journal of Hazardous Materials,* **123**, 135-144, doi:10.1016/j.jhazmat.2005.03.032

Thomas H. (1944), Heterogeneous ion exchange in a flowing system. *Journal of the American Chemical Society*, **66**, 1664-1666, doi: 10.1021/ja01238a017

Uddin M., Rukanuzzaman M., Khan M. and Islam M. (2009), Adsorption of methylene blue from aqueous solution by jackfruit (Artocarpus heteropyllus) leaf powder: A fixed-bed column study. *Journal of Environmental Management*, **90**, 3443-3450, doi:10.1016/j.jenvman.2009.05.030

Víctor-ortega M., Ochando-pulido J. and Martínez A. (2016), Modeling of Fixed Bed Column Studides for Iron Removal from Industrial Effluents through Ion Exchange Process. *Chemical Engineering Transactions,* **47**, 277-282, doi:10.3303/CET1647047

Vieira M., Neto A., Silva M., Carneiro C. and Filho A. (2014), Adsorption of Lead and Copper Ions From Aqueous Effluents on Rice Husk Ash in a Dynamic System. *Brazilian Journal of Chemical Engineering*, **31**, 519-529, doi:10.1590/0104-6632.20140312s00002103

Yoon Y. and Nelson J. (1984), Application of gas adsorption kinetics I. A theoretical model for respirator cartridge service life. *American Industrial Hygiene Association Journal*, **45**, 509-516. http://dx.doi.org/10.1080/15298668491400197